Pore Size Analysis of Activated Carbons from Argon and Nitrogen Porosimetry Using Density Functional Theory

Robert J. Dombrowski, Daniel R. Hyduke, and Christian M. Lastoskie*

Department of Chemical Engineering, Michigan State University, East Lansing, Michigan 48824-1226

Received June 24, 1999. In Final Form: December 28, 1999

We present isotherms calculated from density functional theory for the adsorption of argon in model slit-shaped carbon pores at 77 K. The model isotherms are used to interpret experimental argon uptake measurements and to obtain the pore size distributions of several porous carbons. A similar set of density functional theory isotherms, previously reported for nitrogen adsorption on carbon slit pores at 77 K, are used to determine pore size distributions for the same set of carbons. The pore size distribution maxima, mean pore widths, and specific pore volumes measured using the two different probe gases are all found to agree to within approximately 8% on average. Some of the differences in the pore size distributions obtained from argon and nitrogen porosimetry may be attributable to quadrupolar interactions of the nitrogen molecules with functional groups on the carbon surface.

1. Introduction

Activated carbons are used in the chemical process industries as gas storage media and as selective adsorbents for the separation and purification of vapor- and liquid-phase mixtures. The thermodynamic behavior of a fluid, or a fluid mixture, adsorbed in an activated carbon depends principally on the pore size distribution (PSD) of the adsorbent. Characterization of the PSD is therefore an important problem in industrial applications involving the use of activated carbons.

Commercial activated carbons are manufactured by thermolytic decomposition of various feedstock materials, including cellulosic matter and synthetic polymer resins. The carbonized thermolysis products are "activated" via exposure to steam or carbon dioxide to develop the accessible internal pore volume of the adsorbent.[1] This method of manufacture yields activated carbons that have semiamorphous microstructures. Although such materials defy a simple topological description, we might envision a "typical" activated carbon as a contiguous network of graphitic microcrystals, joined along their edges by surface functional groups, with each crystal containing on the order of 200 atoms, stacked into two or three graphite layers.[2] The size, shape, and connectivity of the pores in an activated carbon depend in a complex manner on the feedstock material used, the temperature and duration of the carbonization, and the extent of steam or CO_2 activation. At present, the relationship between the processing conditions and the resultant carbon structure is poorly understood.

Unlike crystalline adsorbents such as zeolites, or templated porous materials such as MCM-41 mesoporous molecular sieves, activated carbons are not readily characterized by X-ray diffraction or by neutron scattering. Rather, the PSD of a carbon is generally determined indirectly through interpretation of gas adsorption measurements.[3] Extracting PSD information from the experimental adsorption isotherm requires that we make several assumptions regarding the structure of the adsorbent, thus rendering the solution of the PSD numerically tractable. Usually, it is assumed that the activated carbon is composed of noninterconnected, slit-shaped pores with chemically homogeneous, graphitic surfaces. By invoking these assumptions, one can determine the PSD of an activated carbon, $f(H)$, by solving the adsorption integral equation

$$\Gamma(P) = \int_{H_{\min}}^{H_{\max}} \Gamma(P, H)\, f(H)\, \mathrm{d}H \qquad (1)$$

where $\Gamma(P)$ is the specific excess adsorption at bulk gas pressure P, $\Gamma(P, H)$ is the specific excess adsorption at pressure P in a model graphitic slit pore of physical pore width H, and the lower and upper integration limits $H_{\min}$ and $H_{\max}$ correspond to the smallest and largest pore widths that are present in the adsorbent. The value of the PSD function, $f(H)$, at width H represents the total volume of all pores having widths between H and $H + \mathrm{d}H$.

To obtain accurate results for the adsorbent PSD, a realistic pore-filling model must be employed to construct the model isotherms $\Gamma(P, H)$ that appear on the right-hand side of eq 1. Recently, we reported a thermodynamic model for nitrogen adsorption on graphitic slit pores based upon density functional theory (DFT).[4] Comparisons of DFT results to Monte Carlo molecular simulations have shown that the DFT model accurately describes the density profile of the inhomogeneous adsorbed fluid within carbon slit pores.[5] DFT thus provides correct model adsorption isotherms for use in eq 1, at a small fraction of the computational time needed to obtain the same isotherms from molecular dynamics or Monte Carlo molecular simulation. Other, simpler methods that predate DFT,

* To whom correspondence should be addressed. E-mail: cml@msu.edu.

(1) Yang, R. T. *Gas Separation by Adsorption Processes*; Butterworth: Boston, MA, 1987.

(2) Bonsal, R.; Donnet, J.; Stoeckli, F. *Active Carbon*; Marcel Dekker: New York, 1988.

(3) Gregg, S. J.; Sing, K. S. W. *Adsorption, Surface Area and Porosity*; Academic Press: New York, 1982.

(4) Lastoskie, C.; Gubbins, K. E.; Quirke, N. *J. Phys. Chem.* **1993**, *97*, 4786.

(5) Lastoskie, C.; Gubbins, K. E.; Quirke, N. *Langmuir* **1993**, *9*, 2693.

10.1021/la990827a CCC: $19.00
Published on Web 04/27/2000

such as those based on the Kelvin equation[6] and the Horvath−Kawazoe (HK) equation,[7] have also been frequently used as pore-filling models. However, it has been convincingly demonstrated that these classical pore-filling models do not provide a realistic description of adsorption in micropores, and therefore they are not suitable for micropore size characterization.[8,9] Moreover, the classical models are limited in the scope of their applicability, e.g., the Kelvin equation for mesopores and the HK method for micropores, whereas the DFT pore-filling model describes adsorption over the entire range of carbon pore sizes.

Nitrogen is the probe gas most commonly used for PSD analysis because it is inexpensive, readily obtained, inert, and well-studied in the adsorption literature. The experimental isotherm on the left-hand side of eq 1 is usually measured at the normal liquid nitrogen boiling point of 77 K, which is sufficiently below the critical temperature so that a large uptake of the adsorbate is realized. This is again a convenient choice, since liquid nitrogen is inexpensive and isothermal conditions can easily be maintained using liquid nitrogen as a cryostat. Despite these merits, there may arise situations in which a probe gas species other than nitrogen is desirable. On activated carbons that have substantial chemical heterogeneity, there may be significant interactions between the quadrupolar nitrogen molecule and various functional groups (e.g., carboxylic acids) on the carbon surface. The DFT model for nitrogen adsorption does not account for the nonspherical shape of the nitrogen molecule, nor does it allow for possible electrostatic interactions of nitrogen molecules with the carbon surface. The neglect of these features may result in errors in the calculation of the carbon PSD.

Argon is an ideal probe gas for characterizing the pore structure of heterogeneous adsorbents, since it is a monatomic, spherical molecule with no multipolar moments and it is similar in size to nitrogen. Argon porosimetry has been used extensively for PSD analysis of activated carbons, silicas, aluminas, and mesoporous oxides.[3,10] DFT model isotherms have been computed for argon adsorption at its normal boiling point of 87 K.[11] This temperature is readily maintained by using liquid argon as the temperature bath for the sorption measurement. Because liquid argon is more expensive than liquid nitrogen, however, it is convenient and economical to carry out the argon adsorption measurement at the normal liquid nitrogen boiling point of 77 K. Therefore, in this work we present a DFT model for argon adsorption in graphitic slit pores at 77 K. This model is described in section 2, and the model isotherms are reported in section 3. We then compare and analyze, in section 4, the PSD results obtained for several activated carbons, using the argon and nitrogen DFT models to interpret experimental argon and nitrogen isotherms measured on the carbon adsorbents.

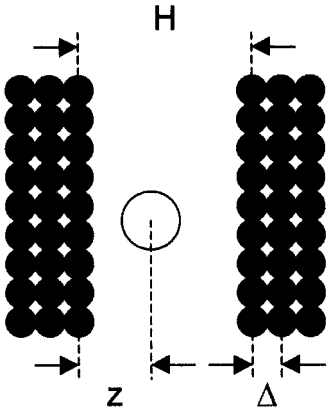

Figure 1. Schematic of a graphitic slit pore model showing the definition of physical pore width H.

2. Theoretical Section: Density Functional Theory

A detailed description of the DFT method has been presented elsewhere,[4] and so we will provide a short summary of the theory. In the DFT method, the local density profile $\rho(\mathbf{r})$ of the inhomogeneous adsorbed fluid at phase equilibrium is determined by solving for the density profile that minimizes the grand potential functional Ω of the confined fluid. The grand potential functional is given as

$$\Omega[\rho(\mathbf{r})] = F[\rho(\mathbf{r})] - \int \mathrm{d}\mathbf{r}\, \rho(\mathbf{r})\, [\mu - V_{\mathrm{ext}}(\mathbf{r})] \qquad (2)$$

where F is the Helmholtz free energy functional, μ is the chemical potential, and V_{ext} is the adsorbate-solid potential at spatial coordinate $\mathbf{r}$. The integration in eq 2 is taken over the entire pore volume of the adsorbent. In a slit pore of physical pore width H, located between two homogeneous graphitic slabs that are unbounded in the lateral directions (Figure 1), the external potential V_{ext} depends only upon one spatial coordinate, the distance z of the adsorbate center-of-mass from the adsorbent surface:

$$V_{\mathrm{ext}}(z) = \phi_{\mathrm{sf}}(z) + \phi_{\mathrm{sf}}(H - z) \qquad (3)$$

In eq 3, ϕ_{sf} is the potential of adsorbate interaction with one of the bounding slabs and H is the separation distance between the carbon nuclei in the surface graphite layers of the opposing pore walls. For a solid density $\rho_s = 0.114$ Å^{-3} and a graphite lattice plane spacing $\Delta = 3.35$ Å, the adsorbate-solid potential is well-represented by the 10−4−3 potential[12]

$$\phi_{\mathrm{sf}} = 2\pi\epsilon_{\mathrm{sf}}\rho_s\sigma_{\mathrm{sf}}^2\Delta\left[\frac{2}{5}\left(\frac{\sigma_{\mathrm{sf}}}{z}\right)^{10} - \left(\frac{\sigma_{\mathrm{sf}}}{z}\right)^4 - \frac{\sigma_{\mathrm{sf}}^4}{3\Delta(z + 0.61\Delta)^3}\right] \qquad (4)$$

where σ_{sf} and ϵ_{sf} are the Lennard-Jones parameters for the adsorbate molecule interaction with a carbon atom in the porous solid. In eq 4, the lateral structure of the graphite layers has been replaced with an integration over the lattice plane surface area (assuming a spatially uniform carbon atom density) and a summation of the layers in each slab. This approximation conveniently reduces the DFT grand potential minimization to a one-dimensional solution of the adsorbate density profile $\rho(z)$.

The Helmholtz free energy functional is computed from perturbation theory as the sum of the hard-sphere Helmholtz free energy functional F_h (for the repulsive

(6) Barrett, E. P.; Joyner, L. G.; Hallenda, P. P. *J. Am. Chem. Soc.* **1951**, *73*, 373.
(7) Horvath, G.; Kawazoe, K. *J. Chem. Eng. Jpn.* **1983**, *16*, 474.
(8) Lastoskie, C.; Quirke, N.; Gubbins, K. E. In *Equilibria and Dynamics of Gas Adsorption on Heterogeneous Solid Surfaces*; Rudzinski, W., Steele, W. A., Zgrablich, G., Eds.; Elsevier: Amsterdam, 1997; Vol. 104, p 745.
(9) Ravikovitch, P. I.; Haller, G. L.; Neimark, A. V. *Adv. Colloid Interface Sci.* **1998**, *76*, 203.
(10) Ravikovitch, P. I.; Haller, G. L.; Neimark, A. V. In *Mesoporous Molecular Sieves*; Rudzinski, W., Bonneviot, L., Beland, F., Danumah, C., Giasson, S., Kaliaguine, S., Eds.; Elsevier: Amsterdam, 1998; Vol. 117, p 77.
(11) Olivier, J. P. *Carbon* **1998**, *36*, 1469.
(12) Steele, W. A. *Surf. Sci.* **1973**, *36*, 317.

adsorbate−adsorbate interactions) and a mean field contribution for the dispersion interactions:

$$F[\rho(\mathbf{r})] = F_h[\rho(\mathbf{r}), d] + {}^1/_2 \int\int d\mathbf{r}\, d\mathbf{r}'\, \rho(\mathbf{r})\, \rho(\rho')\, \phi_{att}(|\mathbf{r} - \mathbf{r}'|) \quad (5)$$

The first term in eq 5 is calculated for hard spheres of diameter d, and the attractive fluid−fluid potential ϕ_{att} in the second term is obtained from the Weeks−Chandler−Andersen representation[13]

$$\phi_{att}(|\mathbf{r} - \mathbf{r}'|) = \phi_{ff}(|\mathbf{r} - \mathbf{r}'|) \qquad |\mathbf{r} - \mathbf{r}'| > r_m$$
$$-\epsilon_{ff} \qquad |\mathbf{r} - \mathbf{r}'| < r_m \quad (6)$$

where $r_m = 2^{1/6}\sigma_{ff}$ and ϕ_{ff} is the Lennard-Jones potential for a pair of adsorbate molecules whose centers of mass are separated by a distance r:

$$\phi_{ff}(r) = 4\epsilon_{ff}\left[\left(\frac{\sigma_{ff}}{r}\right)^{12} - \left(\frac{\sigma_{ff}}{r}\right)^{6}\right] \quad (7)$$

The parameters σ_{ff} and ϵ_{ff} are the Lennard-Jones molecular diameter and well depth for the adsorbate−adsorbate pair potential.

The hard-sphere Helmholtz free energy functional in eq 5 is divided into an ideal and an excess component:

$$F_h[\rho(\mathbf{r}), d] = kT \int d\mathbf{r}\, \rho(\mathbf{r})\, [\ln(\Lambda^3 \rho(\mathbf{r})) - 1] + kT \int d\mathbf{r}\, \rho(\mathbf{r})\, f_{ex}[\bar{\rho}(\mathbf{r}), d] \quad (8)$$

In eq 8, the first term on the right-hand side represents the ideal gas contribution to the hard-sphere free energy; $\Lambda = h/(2\pi mkT)^{1/2}$ is the thermal wavelength, T is the temperature, m is the adsorbate molecular mass, and h and k are the Planck and Boltzmann constants, respectively. The excess molar Helmholtz free energy, f_{ex}, which appears in the second term on the right-hand side of eq 8, is calculated using a *nonlocal* or "smoothed" density profile $\bar{\rho}(\mathbf{r})$ instead of the local adsorbed fluid density profile $\rho(\mathbf{r})$. It is known from surface force microscopy measurements that fluids adsorbed within micropores have highly structured density profiles due to confinement effects.[14] The high degree of fluid ordering at the pore wall surface results in an oscillatory density profile that dampens toward the center of the pore. Similar density profiles have also been observed in molecular simulation studies of fluids confined in micropores.[5] The DFT model does not yield an oscillatory density profile from the minimization of the grand potential functional, however, if the local density profile is used in the calculation of the excess Helmholtz free energy. A relatively unstructured density profile is obtained in the local version of DFT; such a profile is inconsistent with experimental and molecular simulation results.

To properly represent the excess free energy of the adsorbed fluid in eq 8, the density profile that is input to the f_{ex} functional must be weighted so as to account for the sharp spatial gradients in the confined fluid density. A smoothed input density profile is therefore calculated as

$$\bar{\rho}(\mathbf{r}) = \int d\mathbf{r}'\, \rho(\mathbf{r}')\, w[|\mathbf{r} - \mathbf{r}'|, \bar{\rho}(\mathbf{r})] \quad (9)$$

Various prescriptions for the weighting function w have been proposed.[15] In this work, we adopt the weighting function suggested by Tarazona; a detailed description of this nonlocal version of DFT can be found elsewhere.[16] The excess Helmholtz free energy is obtained from the Carnahan−Starling equation of state for a hard-sphere fluid,[17] with an equivalent hard-sphere diameter d given by the Barker−Henderson diameter.[18]

Adsorption isotherms for pores of different widths H are constructed by solving for the adsorbate density profiles $\rho(z)$ that minimize the grand potential functional of the adsorbed fluid over a range of chemical potential values μ. The specific excess adsorption $\Gamma(P, H)$ is then obtained from the line average of the density profile across the width of the pore:

$$\Gamma(P, H) = \frac{1}{H}\int_0^H [\rho(z) - \rho_b]\, dz \quad (10)$$

where $\rho(z)$, ρ_b, and P are the density profile, bulk gas density, and pressure at chemical potential μ. The bulk fluid equations of state that relate ρ_b, P, and μ are given by the set of mean-field equations

$$\mu(\rho_b) = \mu_h(\rho_b, d) + a\rho_b \quad (11)$$

$$P(\rho_b) = P_h(\rho_b, d) + {}^1/_2 a\rho_b^2 \quad (12)$$

where μ_h and P_h are the Carnahan−Starling hard-sphere chemical potential and pressure,[17] respectively, and a is the van der Waals attractive parameter

$$a = 4\pi \int_0^\infty r^2 \phi_{att}(r)\, dr \quad (13)$$

In the argon and nitrogen adsorption experiments (reported in the next section), helium adsorption is used to calibrate the pore volume. This helium-calibrated pore volume is then used to convert the absolute adsorption to an excess adsorption, by subtracting the product of the bulk gas density and the calibrated pore volume from the absolute adsorption. Neimark and Ravikovitch have noted that the same convention should be used in calculating excess adsorption isotherms from DFT for comparison with experimental results.[19] They used DFT to compute a helium-calibrated pore volume and found that the excess isotherms calculated for supercritical methane adsorption in carbon slit pores decrease by 4−5% when the correction for the pore volume is applied. In the case of argon or nitrogen adsorption at 77 K, the correction for the helium-calibrated pore volume is negligibly small (less than 2%), except in slit pores of physical width smaller than 6 Å. Pores that are this narrow exclude argon and nitrogen and are thus inaccessible to PSD analysis using argon or nitrogen porosimetry. We may therefore use eq 10, rather than the helium-calibrated DFT pore volume, in calculating the specific excess adsorption with minimal error.

3. Experimental Section: Argon and Nitrogen Porosimetry

Argon and nitrogen isotherms were measured on four porous carbons at 77 K. The selected carbons were Aldrich

(13) Weeks, J. D.; Chandler, D.; Andersen, H. C. *J. Chem. Phys.* **1971**, *54*, 5237.
(14) Israelachvili, J. N. *Intermolecular and Surface Forces*; Academic Press: London, 1992.
(15) Evans, R. In *Inhomogeneous Fluids*; Henderson, D., Ed.; Marcel Dekker: New York, 1992; Chapter 5.
(16) Tarazona, P. *Phys. Rev. A* **1985**, *31*, 2672; **1985**, *32*, 3148. Tarazona, P.; Marini Bettolo Marconi, U.; Evans, R. *Mol. Phys.* **1987**, *60*, 5743.
(17) Carnahan, N. F.; Starling, K. E. *J. Chem. Phys.* **1969**, *51*, 635.
(18) Barker, J. A.; Henderson, D. *J. Chem. Phys.* **1967**, *47*, 4714.
(19) Neimark, A. V.; Ravikovitch, P. I. *Langmuir* **1997**, *13*, 5148.

Table 1. Lennard-Jones Potential Parameters for Nitrogen[5] and Argon Used in the DFT Model

	argon		
parameter	supercooled liquid	solid	nitrogen
σ_{ff} (Å)	3.375	3.270	3.572
ϵ_{ff}/k (K)	110.2	113.4	93.98
σ_{sf} (Å)	3.362	3.310	3.494
ϵ_{sf}/k (K)	58.02	61.54	53.22

powdered activated carbon 16155-1, granular activated carbon 4021-s, a 100−200 mesh Saran char, and a 50−200 mesh coconut char. An argon isotherm was also measured on Sterling FT, a nonporous graphitized carbon, to obtain the solid−fluid potential parameters for argon adsorption in the model graphitic slit pores. All samples were outgassed at 350 °C for a period of at least 20 h; in all cases, ultimate pressures below 10^{-5} Torr were achieved. Samples were then transferred to an insulated Dewar flask containing a temperature bath of liquid nitrogen. Isothermal conditions at 77.3 ± 0.1 K were maintained during all experiments. Argon and nitrogen adsorption isotherms were measured using a Coulter Omnisorp 100 automated system, over a pressure range from approximately $10^{-5}P_0$ to $0.8P_0$, where P_0 is the bulk saturation pressure of the adsorbate. The specific excess adsorption isotherm is obtained from the absolute amount of gas adsorbed by correcting for the bulk gas density using helium calibration of the pore volume. All isotherms are reported in terms of relative pressure P/P_0. For liquid nitrogen at 77 K, $P_0 = 762 \pm 2$ Torr; for argon at 77 K, the experimental value of P_0 was found to be 204 ± 4 Torr, which is the saturation pressure of solid argon.

4. Fitting of the DFT Model Parameters

The Lennard-Jones parameters σ_{ff} and ϵ_{ff} for bulk nitrogen have been previously fitted[5] to match the saturated liquidnitrogen density of 0.028 87 mol/cm^3 at its normal boiling point of 77.347 K. The fitted parameters are listed in Table 1. The triple-point temperature of bulk argon is 83.8 K; hence, at 77 K, one may elect to fit the bulk argon Lennard-Jones parameters to either the solid argon (0.0411 mol/cm^3; 205 Torr) or the supercooled liquid argon (0.0365 mol/cm^3; 229 Torr) density and saturation pressure.[20] In this work, we have chosen to fit the model parameters using the physical properties of supercooled liquid argon; this yields the fitted values listed in Table 1. Equations 11 and 12 describe only vapor−liquid coexistence and cannot predict the vapor−solid phase coexistence of bulk argon at 77 K. However, the saturation pressure of supercooled liquid argon calculated from eqs 11 and 12 has been found to agree well with the experimental saturation pressure obtained by extrapolating the saturated liquid coexistence line below the argon triple point.[21] It should also be noted that DFT is incapable of predicting solid-phase transitions; hence, the condensed-phase density profiles computed from DFT for argon adsorption at 77 K correspond to supercooled liquid argon, not solid argon. In principle, this mismatch between the theoretical model and the experimental isotherms (which indicate that solid argon condenses in the carbon pores) may cause errors in the PSD analysis. As we shall later demonstrate, however, the computed DFT isotherms are largely unaffected by the choice of the condensed argon phase, and so the effect of this choice on the PSD analysis will be minimal.

(20) *CRC Handbook of Chemistry and Physics*, 61st ed.; Weast, R., Ed.; CRC Press: West Palm Beach, FL, 1981.

(21) Neimark, A. V.; Ravikovitch, P. I.; Grun, M.; Schuth, F.; Unger, K. K. *J. Colloid Interface Sci.* **1998**, *207*, 159.

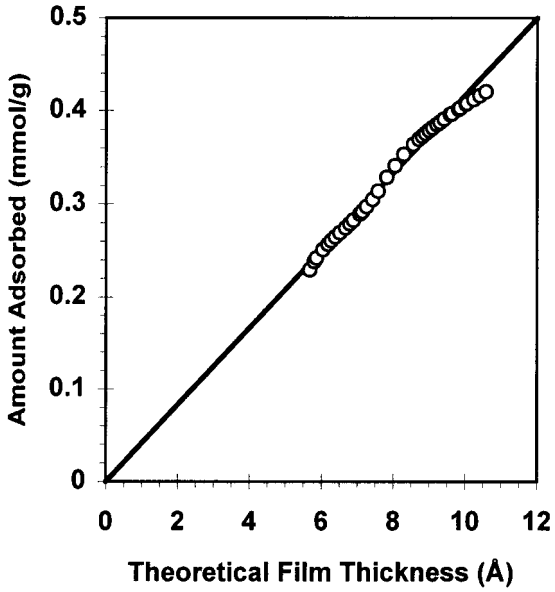

Figure 2. Evaluation of the specific surface area of Sterling nonporous carbon from comparison to the universal film thickness curve. The circles are the experimental isotherm; the solid line shows the linear fit of the data through the origin. The slope of this fitted line yields the specific surface area.

The Lennard-Jones parameters σ_{sf} and ϵ_{sf} for the interaction of adsorbed nitrogen with carbon atoms in a graphite surface have been previously fitted[5] to the nitrogen adsorption isotherm on the nonporous graphitized carbon Vulcan at 77 K (parameter values listed in Table 1). We follow a similar procedure for fitting the parameters of the argon−carbon interaction potential. The argon−carbon effective intermolecular diameter is set equal to the arithmetic mean of the argon−argon and carbon−carbon molecular diameters. The Lennard-Jones well depth ϵ_{sf} for the argon−carbon interaction is then determined by selecting the value that provides the best quantitative agreement between the experimental argon isotherm of the nonporous reference carbon and the DFT isotherm for argon adsorption in a model graphitic slit pore of width $H = 67.5$ Å. This mesopore is sufficiently large so that the adsorbed films on the two opposing surfaces of the slit pore have no significant potential interactions; i.e., at low relative pressures, the DFT isotherm in this slit pore can be regarded as the adsorption isotherm on two isolated (nonporous) graphite surfaces. To directly compare the experimental and DFT model isotherms, we must first determine the specific surface area of the reference carbon, which in the case of argon is a Sterling FT graphitized carbon. Following the method of de Boer et al.,[22] the specific surface area is obtained by fitting a line through a plot of the argon uptake versus the theoretical film thickness (Figure 2). A specific surface area of 11.3 m^2/g was measured for the Sterling carbon; this value was then used to convert the DFT-calculated specific excess argon adsorption in the 67.5-Å-slit pore from a pore volume basis to an adsorbent mass basis, as described in our previous work.[5] The well-depth parameter ϵ_{sf} that yielded the best agreement between the DFT model and the experimental argon isotherm is reported in Table 1, and a comparison of the experimental isotherm and the fitted DFT isotherm is shown in Figure 3. The best-fit value of ϵ_{sf} was considered to be the one for which the low-pressure inflection point in the DFT isotherm, corresponding to the formation of an adsorbed

(22) de Boer, J. H.; Linsen, B. G.; Osinga, T. J. *J. Catal.* **1965**, *4*, 643.

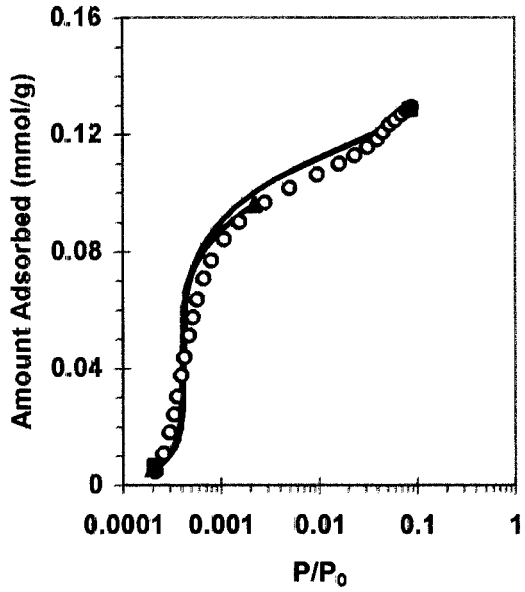

Figure 3. Argon adsorption on nonporous carbon surface at 77 K. The circles are the experimental isotherm measured on Sterling FT graphitized carbon. The lines are the DFT-fitted isotherms in a model graphitic slit pore of width $H = 67.5$ Å, obtained using the Lennard-Jones potential parameters calculated from the supercooled liquid (square end points) and solid (triangle end points) argon bulk physical properties.

monolayer, most closely matched the inflection point in the monolayer region of the experimental isotherm.

It has been found that the DFT isotherm always exhibits a greater slope around this inflection point than the experimental isotherm. This is to be expected, since the DFT isotherm is based upon adsorption on a homogeneous model graphitic surface, whereas the Sterling reference carbon, and any other nonporous carbon, will retain some degree of surface heterogeneity, no matter what the extent to which the adsorbent is graphitized. Surface physical and/or chemical heterogeneities broaden the site energy distribution of the adsorbent surface and cause the measured isotherm to have a shallower slope than it would if the surface were energetically homogeneous.[23] It should also be noted that we have deliberately chosen to fit the solid−fluid potential parameters to the monolayer region of the nonporous reference isotherm and have not attempted to obtain quantitative agreement between the DFT isotherm and the experimental isotherm at higher relative pressures. At low relative pressures (i.e., $P/P_0 < 10^{-3}$), the principal potential interactions are between the argon molecules and the surface carbon atoms, whereas at higher pressures, argon−argon interactions become more substantial as the adsorbed films thicken. It is generally not possible to fit the multilayer/condensation region of the nonporous (BET-type) isotherm at $P/P_0 > 0.4$ using the DFT model because the model isotherm will exhibit a condensation-phase transition at a relative pressure specific to the pore slit width. This lack of agreement, however, is inconsequential to the fitting of the Lennard-Jones solid−fluid potential parameters, which can be accomplished very satisfactorily using only the low-pressure portion of the reference isotherm.

5. DFT Model Isotherms for Carbon Slit Pores

In Figure 4, the model DFT isotherms are shown for argon adsorption in graphitic slit pores at 77 K, calculated

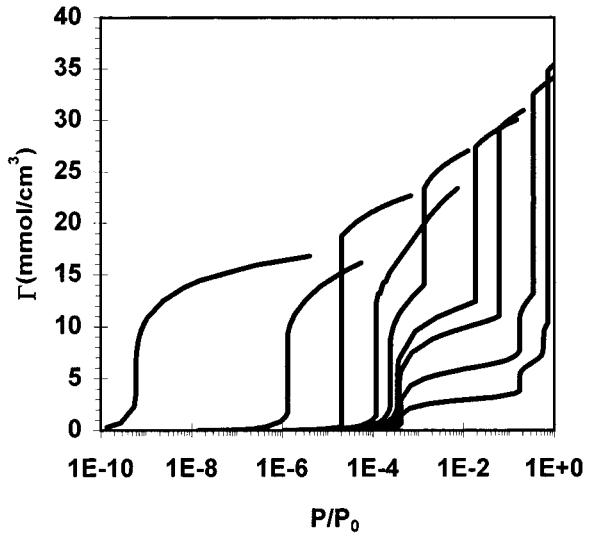

Figure 4. Argon specific excess adsorption in model graphitic slit pores at 77 K, calculated from DFT. Isotherms are shown for slits having physical pore widths H (reading from left to right) of 6.8, 8.4, 10.5, 11.8, 13.5, 16.9, 20.2, 33.8, and 67.5 Å.

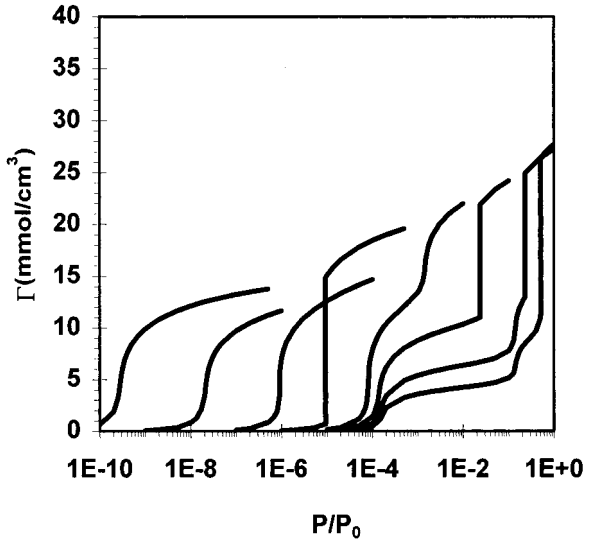

Figure 5. Nitrogen specific excess adsorption in model graphitic slit pores at 77 K, calculated from DFT.[5] Isotherms are shown for slits having physical pore widths H (reading from left to right) of 7.1, 8.0, 8.9, 10.7, 13.4, 17.9, 28.6, and 42.9 Å.

using the potential parameters summarized in Table 1. For comparison, the DFT isotherms for nitrogen adsorption at 77 K in pores over the same size range are presented in Figure 5. The overall shapes of the argon and nitrogen isotherms are similar: in the micropores, the pores fill in a single step, whereas, in the mesopores, condensation is preceded by the formation of a monolayer, and, in the larger slit pores, condensation is preceded by wetting of one or more additional adsorbed layers. There are some notable differences between the argon and nitrogen DFT isotherms. In the nitrogen adsorption model, the isotherms of the micropores smaller than 10 Å are continuous, whereas, for the argon model, a phase transition is predicted in these pores. In the pores larger than 14 Å, the nitrogen model predicts continuous pore filling during growth of the adsorbed film, followed by a single phase transition at the capillary condensation pressure. The argon DFT isotherms, in contrast, exhibit multiple phase transitions at the monolayer and multilayer filling pressures, in addition to the capillary condensation pressure.

(23) Olivier, J. P. In *Proceedings of the Fifth International Conference on Fundamentals of Adsorption*; LeVan, M. D., Ed.; Kluwer Academic Publishers: Boston, MA, 1996; p 699.

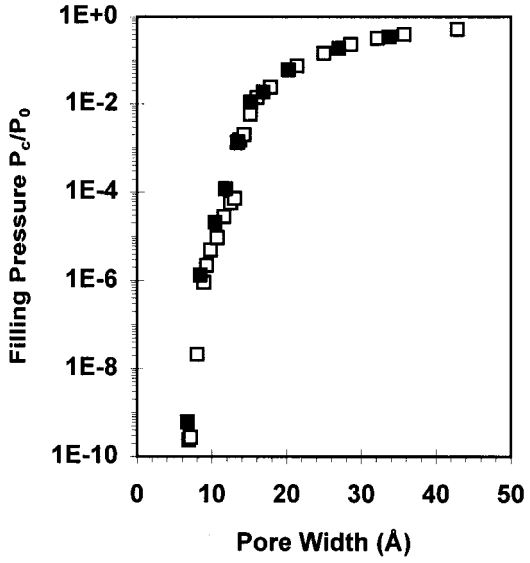

Figure 6. Pore-filling correlation with slit pore width for DFT models of argon and nitrogen adsorption at 77 K: filled squares, argon; open squares, nitrogen.

The more steplike structure of the argon DFT isotherms is not unexpected, since these isotherms are calculated at a lower reduced temperature T/T_c than the nitrogen isotherms. (The critical temperature T_c of argon, obtained from mean-field theory using eqs 12 and 13, is 164.7 K; for nitrogen, it is 140.5 K. Both of these values, it should be noted, are approximately 14 K higher than the actual critical temperatures of the gases, since mean-field theory does not correctly predict the curvature of the liquid−vapor coexistence curve near the critical point.)

The pore-filling pressures are shown as a function of slit pore width in Figure 6 for argon and nitrogen adsorption at 77 K. It can be seen that, for a given pore width, argon and nitrogen condense at nearly the same relative pressure. The adsorbed argon density, however, is greater than the adsorbed nitrogen density when complete pore filling has occurred. (This can be seen by comparing Figures 4 and 5.) A higher adsorbed-fluid density is achieved for argon because it has a smaller molecular diameter than nitrogen and it is adsorbed at a lower reduced temperature than nitrogen.

6. PSD Analysis of Porous Carbons

Experimental argon and nitrogen adsorption isotherms at 77 K are reported in Figures 7−10 for four porous carbons. At saturation, the total excess adsorption of argon exceeds that of nitrogen in all four cases; this is consistent with the predictions of the DFT models shown in Figures 4 and 5.

The adsorption isotherm of each carbon is fitted using the appropriate DFT pore-filling model in eq 1, to obtain the PSD of the adsorbent. For convenience, we have elected to fit the PSD of each carbon to the trimodal Γ distribution ($m = 3$)

$$f(H) = \sum_{i=1}^{m} \frac{\alpha_i(\gamma_i H)^{\beta_i}}{\Gamma(\beta_i)H} \exp(-\gamma_i H) \qquad (14)$$

which has nine adjustable parameters: the amplitude α_i, mean β_i, and variance γ_i of each mode i of the distribution. In eq 14, Γ refers to the Γ function. It is important to note that this choice of a fitting function is completely arbitrary and that there is no physical basis for assuming that the

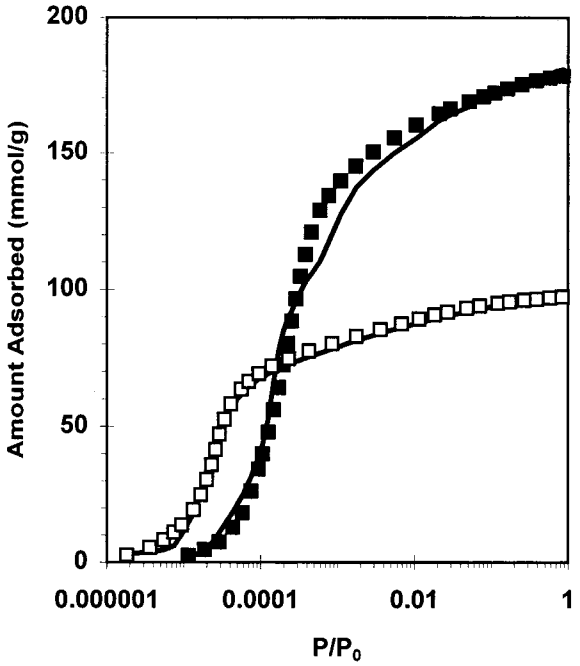

Figure 7. Adsorption isotherms on Saran char at 77 K: filled squares, argon uptake; open squares, nitrogen uptake. The lines show the respective DFT isotherms obtained for argon and nitrogen using the PSD that best fits the DFT model to the experimental isotherm of each probe gas. The PSDs for argon and nitrogen are fitted separately.

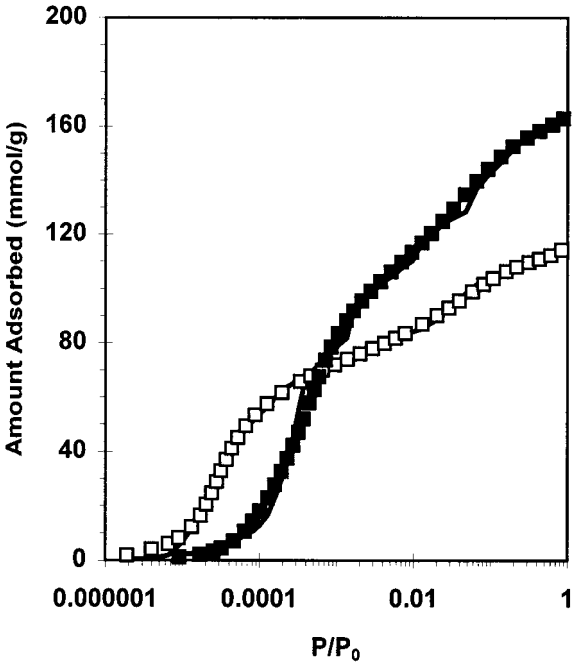

Figure 8. Argon and nitrogen isotherms on coconut char at 77 K. The notation is the same as for Figure 7.

PSD of an adsorbent is uniquely described by the Γ distribution or any other sum of mathematical distributions. There is in fact no need whatsoever to use a distribution function to fit the PSD; an equally valid approach is to subdivide the PSD into several dozen or more pore width increments and assign an independently adjustable amplitude coefficent α_j to each pore width increment j. The only mathematical constraint on the PSD function is that it must be nonnegative for all pore widths H. If the PSD function contains too few adjustable parameters (e.g., a unimodal distribution), the choice of

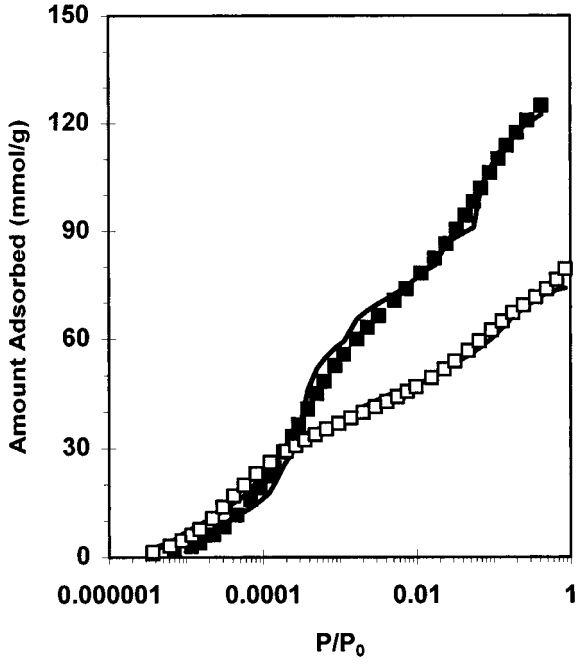

Figure 9. Argon and nitrogen isotherms on granular activated carbon at 77 K. The notation is the same as for Figure 7.

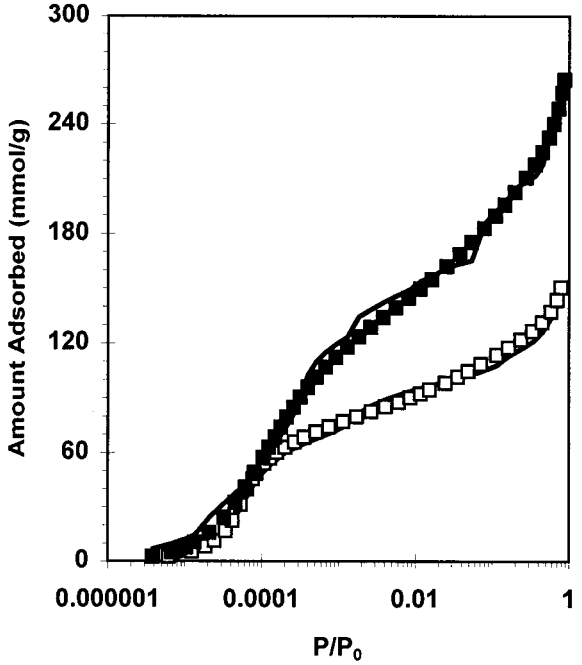

Figure 10. Argon and nitrogen isotherms on powdered activated carbon at 77 K. The notation is the same as for Figure 7.

the fitting function may unduly constrain the PSD results. It has been our experience, however, that a trimodal distribution provides ample flexibility for determining the PSDs of activated carbons. We have previously demonstrated, for example, that the nitrogen adsorption isotherm of a porous carbon can be fit very accurately with the DFT model using either a trimodal Γ distribution or a trimodal log-normal distribution to represent $f(H)$.[4] The PSDs obtained using these two distributions are essentially indistinguishable, underscoring that it is the *numerical values* of the PSD itself that are unique, not the function that is arbitrarily chosen to represent the PSD.

The adsorption integral, eq 1, is evaluated for each probe gas/adsorbent pair using numerical integration. A least-

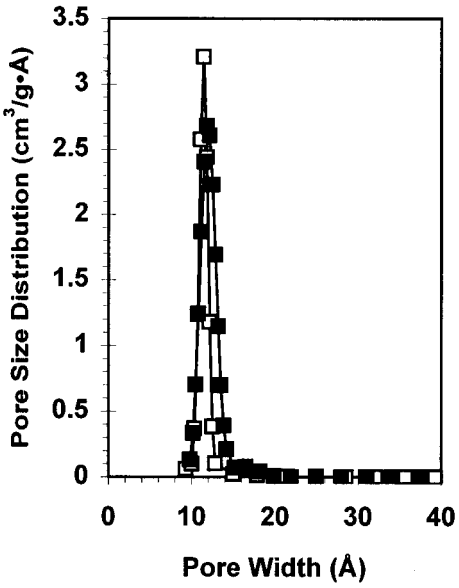

Figure 11. PSDs obtained from argon (filled squares) and nitrogen (open squares) porosimetry for Saran char using the DFT method.

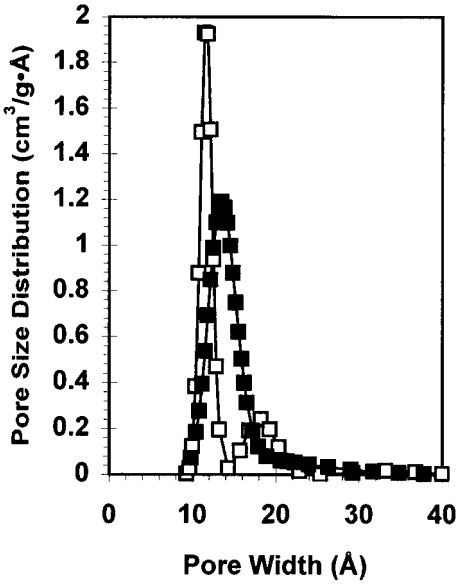

Figure 12. PSDs obtained from argon and nitrogen porosimetry for coconut char using the DFT method. The notation is the same as for Figure 11.

squares error minimization criterion is used to determine the best-fit PSD parameters for each carbon. The best-fit model isotherm for each experimental isotherm is shown as a solid line in Figures 7−10. A comparison of the PSDs that yield the best-fit argon and nitrogen DFT isotherms is shown for each porous carbon in Figures 11−14. We note that a good fit of the DFT model to the experimental data is obtained for all eight measured isotherms. The cases where there are observable differences between the DFT model and the experimental isotherm can be attributed to the model isotherm being more structured than the measured isotherm. This is due to the assumption of physical and chemical homogeneity in the graphitic slit pore model and to the effects of heterogeneity in smoothing the structure of the experimental isotherms. The differences between the DFT fitted isotherms and the experimental results are slightly more pronounced for the set of argon isotherms because of the phase transitions predicted by DFT for this adsorbate at 77 K. Overall,

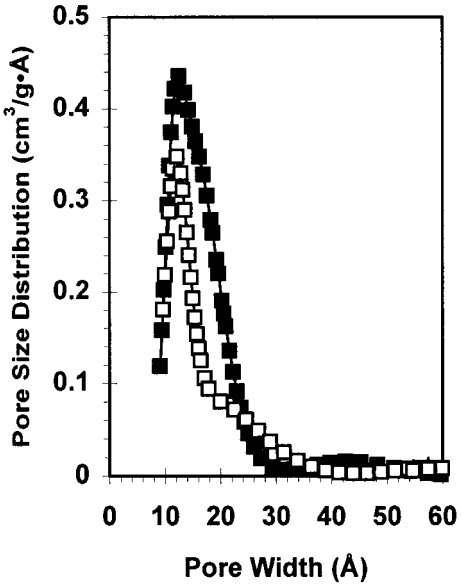

Figure 13. PSDs obtained from argon and nitrogen porosimetry for granular activated carbon using the DFT method. The notation is the same as for Figure 11.

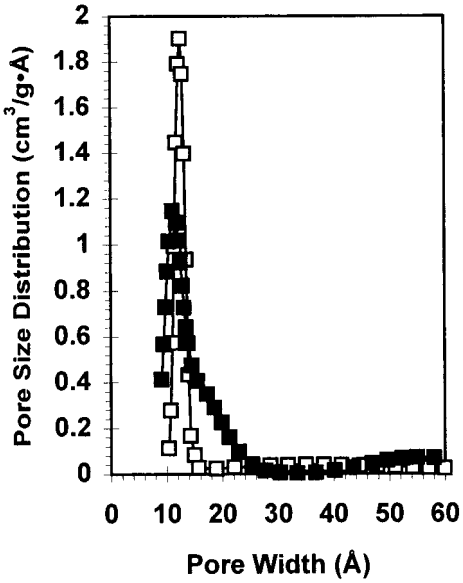

Figure 14. PSDs obtained from argon and nitrogen porosimetry for powdered activated carbon using the DFT method. The notation is the same as for Figure 11.

however, an acceptable fit of each experimental isotherm is obtained using a trimodal Γ distribution for the PSD.

The PSD for each adsorbate/adsorbent pair (Figures 11−14) is truncated at a lower bound corresponding to the width of the slit pore that condenses at the lowest pressure measured in the experimental isotherm. This lower pore size bound is determined from interpolation of the DFT pore-filling correlations shown in Figure 6. Our justification for truncating the PSD is that all the pores that are narrower than the lower bound pore width are already filled with condensate at the start of the experimental isotherm measurement. Consequently, no phase transition will be observed in these pores over the course of the experiment and no information regarding the PSD of these micropores may reliably be obtained. (A slight increase in the condensate density does occur in pores of all sizes as the pressure increases due to compression of the adsorbed fluid; however, this compression effect alone is insufficient to unambiguously determine the PSD of micropores smaller than the lower bound pore width.)

Table 2. PSD Maxima, Mean Pore Widths, and Pore Volumes of the Adsorbent Samples as Determined from DFT Interpretation of Argon and Nitrogen Porosimetry Data

adsorbent	adsorbate	PSD max (Å)	mean pore width (Å)	pore vol (cm^3/g)
Saran char	Ar	11.8	12.2	0.432
	N_2	11.4	10.7	0.487
	% diff	−3.4	−12.0	+12.5
coconut char	Ar	13.5	14.9	0.569
	N_2	11.4	13.9	0.568
	% diff	−15.6	−6.6	−0.2
granular activated carbon	Ar	12.5	17.3	0.488
	N_2	12.9	18.6	0.414
	% diff	+3.2	+7.5	−15.2
powdered activated carbon	Ar	11.1	22.2	0.598
	N_2	12.5	23.3	0.582
	% diff	+12.6	+5.0	−2.5

All four porous carbons have a large micropore volume, as can be seen from the PSD peak exhibited by each adsorbent in the 11−13 Å range. Some mesopore volume also appears to be present in the granular and powdered activated carbons, as evidenced by the broad secondary peak in the PSDs of these samples in the 40−60 Å range. For each of the four samples, the PSD interpreted from the argon porosimetry data has a somewhat broader distribution of pore sizes than the PSD obtained from the nitrogen data. A comparison of the argon and nitrogen results for the pore volume, mean pore width, and maximum in the PSD of each adsorbent is presented in Table 2. The specific pore volume V_p and the mean pore width $\bar{H}$ are calculated as

$$V_p = \int_{H_{min}}^{H_{max}} f(H)\, dH \tag{15}$$

$$\bar{H} = \frac{\int_{H_{min}}^{H_{max}} H\, f(H)\, dH}{V_p} \tag{16}$$

For the char samples, the mean pore width is only slightly larger than the width corresponding to the PSD maximum, whereas, for the activated carbon samples, the mean pore width is substantially larger than the PSD maximum due to the significant mesoporosity of these adsorbents. The percentage difference in the argon and nitrogen values for each adsorbent property is calculated as

$$\%\ \text{difference} = 100\% \times (N_2\ \text{value} - \text{Ar value})/(\text{Ar value}) \tag{17}$$

and is also reported in Table 2. The difference in the PSD maxima measured via argon and nitrogen porosimetry ranges between 3 and 16%, with an average differential of 8.7% for the four samples tested. The differences in the mean pore width and pore volume vary over similar ranges, with average differentials of 7.8 and 7.6%, respectively.

7. Discussion of Argon and Nitrogen Porosimetry Methods

With regard to fluid separation applications, the most important physical property of a porous carbon is the maximum in its PSD. The average differential of 8.7% in the PSD maxima calculated from the argon and nitrogen porosimetry measurements using DFT constitutes may be regarded as reasonably good agreement between the two separate probe gas analyses. This is particularly so, given that the calculation of the PSD is subject to error

resulting from any of three separate inputs: (1) the precision of the experimental isotherm measurement, (2) the accuracy of the DFT pore-filling model, and (3) the soundness of the numerical method used to invert the Fredholm integral of eq 1 to obtain the PSD. Of these three contributing factors, the second is most likely to be responsible for the observed differences in the PSDs computed from the argon and nitrogen adsorption measurements. The construction of the DFT isotherms $\Gamma(P, H)$ used in the solution of $f(H)$ in eq 1 requires that we invoke major simplifications with regard to the structure of the model carbon adsorbent. The assumptions of a slit pore shape and surface homogeneity and the neglect of connectivity are at best crude approximations of the actual structures of the porous carbons studied in this work. Hence, it is to be expected that some inconsistencies will arise in the PSDs calculated from argon and nitrogen porosimetry as a result of the DFT model assumptions (or, for that matter, the assumptions made in any other pore-filling model). In the case of a more ordered adsorbent, such as a mesoporous molecular sieve, we might anticipate better agreement between the argon- and nitrogen-derived PSDs, since our pore model construct for a highly ordered porous material will more closely match the actual pore structure of the adsorbent. For example, excellent agreement was found in PSD results obtained by using DFT to interpret argon and nitrogen adsorption isotherms at 77 and 87 K on MCM-41 type adsorbents, a class of mesoporous molecular sieves that have one-dimensional, cylindrical oxide channels with pore diameters between 32 and 45 Å.[21]

One might then ask the following question: Which of the PSDs obtained, from argon and from nitrogen porosimetry, is the more reliable representation of the actual carbon PSD? There is reason to favor the PSD interpreted from argon porosimetry, on account of the nitrogen quadrupole and possible electrostatic interactions of nitrogen molecules with carbon surface functional groups.

A comparison of Figures 4 and 5 indicates that the argon and nitrogen DFT models both predict that an adsorbed monolayer will form at $P/P_0 \cong 10^{-4}$ in pores larger than 13 Å. In the experimental isotherms of the activated carbons (Figures 9 and 10), the relative pressures at which the argon and nitrogen monolayers form are indeed the same. In the case of the char samples (Figures 7 and 8), however, the nitrogen monolayer forms at a relative pressure nearly a full order of magnitude lower than the argon monolayer. We speculate that the lower relative pressure for nitrogen monolayer filling is the result of quadrupolar interactions of the nitrogen adsorbate with functional groups on the surface of the chars. Argon, which has no permanent multipole, is largely unaffected by the presence of surface functional groups, but nitrogen may adsorb at a lower relative pressure on a chemically heterogeneous surface because of quadrupolar interactions.

Elemental analysis of the carbon, hydrogen, and nitrogen (CHN) content of each adsorbent sample was conducted,[26] and the results are reported in Table 3. It was found that approximately 4−8 wt % of each adsorbent is composed of elements other than CHN. This unidentified fraction is presumably oxygen, with perhaps a small amount of sulfur also present. The oxygen and sulfur atoms are likely to be contained in polar surface functional groups such as carboxylic acids that may interact with the nitrogen quadrupole. Although no explicit correlation with the adsorption isotherm can be inferred from the compositional data of Table 3, the weight fraction of non-CHN elements in the adsorbents is large enough for us to surmise that nitrogen quadrupolar interactions may cause differences in the argon and nitrogen isotherms at low pressure. The quadrupole moment of nitrogen has been previously invoked to explain differences in the site energy distributions of controlled pore glasses calculated from argon and nitrogen adsorption at 77 K[24] and differences in the PSDs of microporous carbons determined from supercritical methane adsorption and subcritical nitrogen adsorption.[25]

Table 3. Elemental Compositions of the Adsorbent Samples[a]

	elemental compd (wt %)			
adsorbent	carbon	hydrogen	nitrogen	other
Saran char	91.2	1.1	3.8	3.9
coconut char	86.6	1.2	3.8	8.5
granular activated carbon	91.2	1.2	3.8	3.8
powdered activated carbon	89.2	1.4	3.5	5.8

[a] The column labeled "other" was calculated by subtracting the measured weight percentages of carbon, hydrogen, and nitrogen from 100%.

Electrostatic interactions are not explicitly accounted for in the DFT pore-filling model, which assumes that the adsorbate molecules are spherically symmetric and interact only via van der Waals (i.e., dispersion/repulsion) forces. If the neglected quadrupolar interactions are substantial, then DFT analysis of the nitrogen isotherm will yield mean pore widths that are too small. This might explain some of the observed differences in the PSDs obtained for the chars.

It is therefore our recommendation that argon porosimetry be used to interpret the PSDs of porous carbons if there is reason to believe that the adsorbent is chemically heterogeneous. While this procedure will not eliminate the effects of other heterogeneities (e.g., surface defect sites or pore junctions) that may be present and that equally affect argon and nitrogen adsorption, it will at a minimum avoid the potentially confounding effects of the nitrogen quadrupole on the analysis of the PSD.

It has been noted that the Lennard-Jones parameters for the argon−argon pair interaction potential can be fit to physical properties of either solid argon or supercooled liquid argon at 77 K. The argon DFT isotherms and PSD results reported in this work were obtained using the supercooled liquid argon properties to fit the model parameters. The saturation pressure measured in the argon adsorption experiments, on the other hand, indicates that solid argon condenses in the porous carbons. To assess the possible errors caused by the mismatch of the condensed argon phase in the theory and experiments, the potential parameters for the argon−argon and argon−carbon interactions were recalculated using the solid argon physical properties by following the same procedure outlined in section 4. The best-fit Lennard-Jones parameters using the solid argon properties as the basis for fitting are summarized in Table 2, and a comparison of the DFT model isotherms, fitted to the Sterling reference isotherm, is shown in Figure 3 for the two different sets of argon potential parameters. It is found that using the solid argon physical properties increases the argon−argon potential well depth by 3% and decreases the argon molecular diameter by the same amount. Using the arithmetic mean for the argon−carbon effective diameter and a recalculated

(24) Olivier, J. P. In *Proceedings of the Sixth International Conference on Fundamentals of Adsorption*; Elsevier: Amsterdam, 1998; p 207.
(25) Quirke, N.; Tennison, S. R. R. *Carbon* **1996**, *34*, 1281.
(26) The elemental analysis was provided by the Michigan State University Hazardous Waste Analysis Laboratory, East Lansing, MI.

specific surface area of 10.1 m^2/g from the thickness curve plot, it is found that the Sterling isotherm is best fit with an argon−carbon well depth that is 6% larger than the well depth fitted from the supercooled liquid data. As can be seen from inspection of Figure 3, however, either set of potential parameters will yield a set of DFT isotherms that reproduces the experimental monolayer-filling pressure of $\sim 10^{-4} P_0$. The only observable difference in the fitted isotherms is in the adsorbed phase density. Thus, the two sets of model parameters will yield different predictions of pore volume, but the location of the PSD maxima (as determined from the pore filling pressure correlation) will be nearly the same for the two argon models. On the basis of the rather small value of σ_{ff} obtained by fitting the parameters to the solid data, and other considerations discussed in section 4, it is our recommendation that the supercooled liquid properties be used to model argon adsorption at 77 K. An alternative, to avoid uncertainty in the parameter fitting, is to conduct the argon experiments and modeling at the normal liquid argon boiling point of 87 K, using liquid argon instead of liquid nitrogen as the temperature bath.

Finally, it should be noted that the PSD results reported in Figures 11−14 are obtained without the use of regularization methods. Regularization refers to a numerical technique whereby additional constraints are specified in order to convert a mathematically ill-posed problem—the solution of the PSD function $f(H)$ in eq 1—into a well-posed problem.[27] The effect of regularization is to "smooth" the PSD by suppressing perturbations caused by experimental error in the isotherm data.[28] Given that we have not used any regularization in solving the adsorption integral equation for the best-fit PSD, the general agreement between the argon and nitrogen results for the PSD maxima is quite good. If regularization were to be utilized, we would expect to find even closer agreement between the argon- and nitrogen-derived PSDs. For example, a large value of the regularization "smoothing" parameter would convert the bimodal PSD fits obtained for some of the carbons into unimodal PSDs. The relatively good agreement between the argon and nitrogen porosimetry results, even in the absence of regularization, may be taken as evidence of the fundamental soundness of the DFT pore-filling model.

8. Conclusion

In this work, we have shown that a DFT model of argon adsorption at 77 K in slit-shaped carbon pores yields PSD results from argon porosimetry that are comparable to PSDs obtained by interpreting nitrogen adsorption at 77 K using a similar DFT model. The specific pore volume, mean pore width, and maximum in the PSD of a carbon adsorbent can be bracketed to within 8%, on average, by comparing the PSDs determined from the two separate probe gas measurements. The DFT model does not account for nitrogen quadrupolar interactions; therefore, divergent PSD results are to be expected if the argon and nitrogen DFT models are used to interpret the isotherms of porous carbons that possess polar surface functional groups. In such cases, it is recommended that argon porosimetry be used in conjunction with the argon DFT model to determine the PSD of the adsorbent.

Acknowledgment. This work was supported by the National Science Foundation through a CAREER award grant (CTS-9733086). We thank the Beckman Coulter Corp. for providing an Omnisorp 100 gas sorption analyzer for the experimental isotherm measurements.

LA990827A

(27) von Szombathely, M.; Brauer, P.; Jaroniec, M. *J. Comput. Chem.* **1992**, *13*, 17.

(28) Davies, G. M.; Seaton, N. A. *Carbon* **1998**, *36*, 1473.